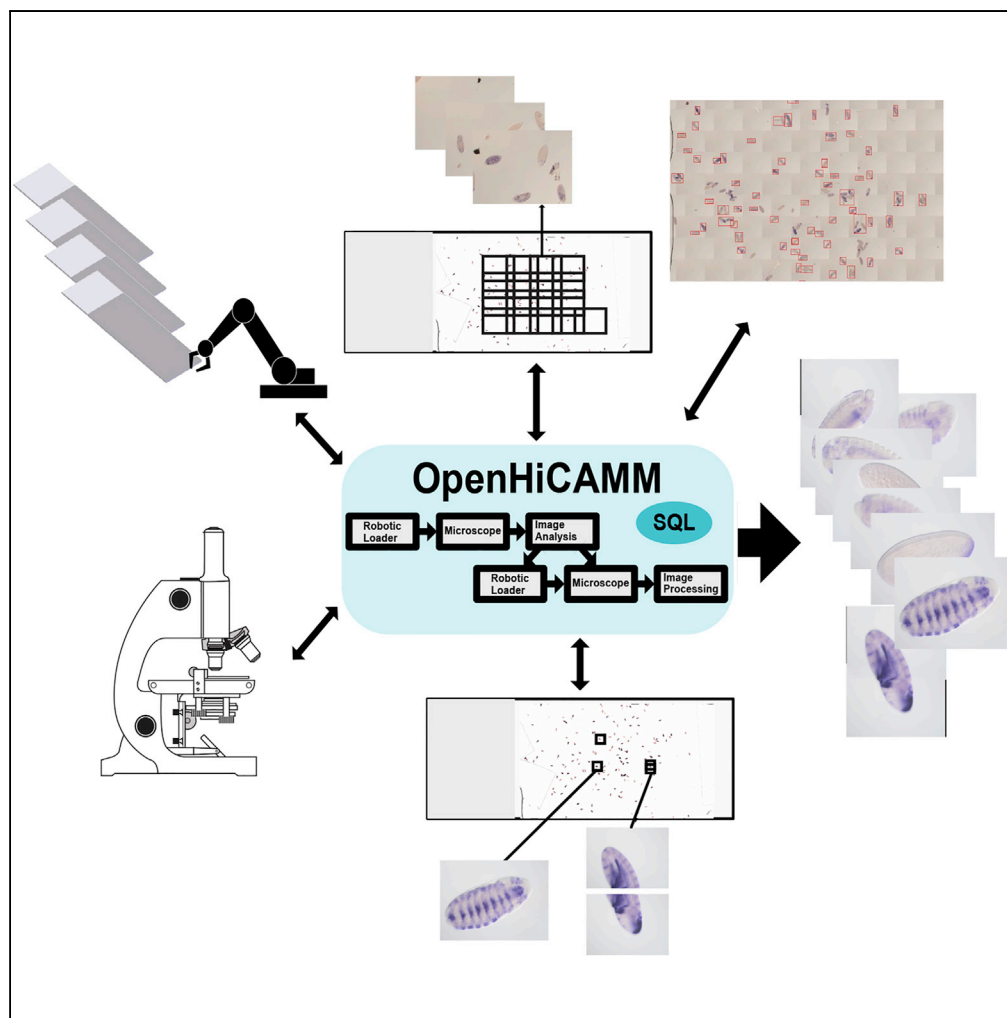


Article

OpenHiCamm: High-Content Screening Software for Complex Microscope Imaging Workflows



Benjamin W. Booth, Charles McParland, Keith Beattie, William W. Fisher, Ann S. Hammonds, Susan E. Celniker, Erwin Frise

erwin@fruitfly.org

HIGHLIGHTS

OpenHiCamm is an open source software that integrates robotics and image acquisition

OpenHiCamm is a module for the Fiji/ImageJ and μ Manager software packages

OpenHiCamm tracks images on multiple slides and controls an optional slide loader

OpenHiCamm is easily adapted for high-throughput screening and image analysis

Booth et al., iScience 2, 136–140
 April 27, 2018 © 2018 The Authors.
<https://doi.org/10.1016/j.isci.2018.03.017>

Article

OpenHiCamm: High-Content Screening Software for Complex Microscope Imaging Workflows

Benjamin W. Booth,¹ Charles McParland,² Keith Beattie,² William W. Fisher,¹ Ann S. Hammonds,¹ Susan E. Celniker,¹ and Erwin Frise^{1,3,*}

SUMMARY

High-content image acquisition is generally limited to cells grown in culture, requiring complex hardware and preset imaging modalities. Here we report an open source software package, OpenHiCamm (Open Hi Content Acquisition for μ Manager), that provides a flexible framework for integration of generic microscope-associated robotics and image processing with sequential workflows. As an example, we imaged *Drosophila* embryos, detecting the embryos at low resolution, followed by re-imaging the detected embryos at high resolution, suitable for computational analysis and screening. The OpenHiCamm package is easy to use and adapt for automating complex microscope image tasks. It expands our abilities for high-throughput image-based screens to a new range of biological samples, such as organoids, and will provide a foundation for bioimaging systems biology.

INTRODUCTION

Large-scale genome sequencing has rapidly facilitated the investigation and analysis of gene and protein functions and interactions. Efforts to interpret sequence data and to understand how they are used to control cellular, tissue, or organ system development have quickly revealed the limitations in our molecular understanding of multicellular organisms. Spatial gene expression is important for understanding the events that are necessary for the development of metazoans, and large-scale studies are underway for a number of species (e.g., Hammonds et al., 2013; Lein et al., 2007; Pollet et al., 2005; Tabara et al., 1996). Indeed, even the existence of uniform cells or tissues has been questioned, and their variance has been masked by single measurements (Levsky and Singer, 2003).

High-content screening (HCS) is routinely used in cell culture imaging, pharmaceutical drug discovery, genome-wide RNA interference (RNAi), and CRISPR (Boutros et al., 2015). Commercial equipment is readily available (Zanella et al., 2010) and able to scan multi-well plates and slides. Commercial automated microscopes are integrated packages of robotics, microscope, and software, limiting possible customizations, especially for well-suited existing microscope systems. Imaging is done in a single pass, requiring a compromise between resolution and field depth. For single cell samples, this means a tradeoff between resolution and cell density. Transient transfections may not have sufficient cell transfection density for high-resolution imaging. For larger samples, such as histological sections, organoids, or whole-mount samples of model organisms or tissues, specimens need to be tiled at low resolution or placed at a predefined position.

We describe new software for high-throughput imaging, specifically designed to automate image acquisition that requires multi-step workflows contingent on image analysis and multiple imaging modalities. The software, OpenHiCamm (Open Hi Content Acquisition for μ Manager) controls optical microscopes and interfaces with an automated slide loader to perform fully automated HCS.

RESULTS

We developed OpenHiCamm as a module for the popular open source bioimage analysis package Fiji (Schindelin et al., 2012) and microscope hardware control μ Manager (Edelstein et al., 2010). OpenHiCamm utilizes μ Manager for its broad support of microscopes, components, and cameras and its flexible slide acquisition. For advanced image analysis, our modules use Fiji's software components. Other existing μ Manager extensions are designed for thorough exploration of single samples (Pinkard et al., 2016; Pitrone et al., 2013), whereas our software is designed to process large sample sets.

¹Biological Systems and Engineering Division, Lawrence Berkeley National Laboratory, Berkeley, CA 94720, USA

²Computer Science Research Division, Lawrence Berkeley National Laboratory, Berkeley, CA 94720, USA

³Lead Contact

*Correspondence: erwin@fruitfly.org

<https://doi.org/10.1016/j.isci.2018.03.017>



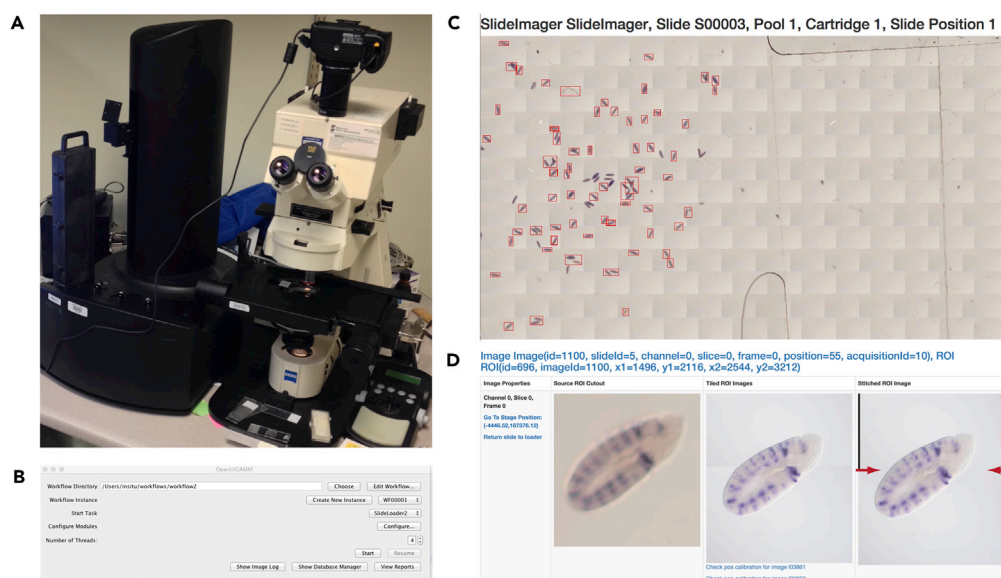


Figure 1. Microscope Setup and OpenHiCamm Results

(A) Microscope with motorized stage (on the right) and the automated slide loader (on the left). (B) Main dialog box for OpenHiCamm, showing the workflow storage directory in use, tabs allowing user configuration options and access to reports and logs. See also [Figure S10–S14](#). (C and D) Excerpts of the OpenHiCamm report. (C) Image of a processed slide, stitched by stage position and the automated detection of regions of interest (ROI) shown boxed in red. (D) Screenshot from the report page showing the results for one detected ROI; (left) the image at 5 \times magnification, (middle) the image at 20 \times magnification superimposed by relative position, (right) the final image at 20 \times magnification stitched with the Fiji's algorithm (red arrows indicate the stitching position). See also [Figure S1](#).

The core of OpenHiCamm is a sophisticated workflow manager that executes modules operating the robotic hardware, performing the imaging and processing the data ([Table S1](#), [Figure S3](#) and [Tables S2–S4](#)). In the spirit of Fiji and μ Manager, we designed a high-quality, open and extensible Java core. The workflow manager executes microscope-dependent modules sequentially and computational processing modules in parallel. OpenHiCamm uses an integrated SQL database engine for persistent storage of workflow setups, for module configurations, and for recording completed tasks, thus allowing for recovery from operational hardware problems and stopping or resuming interrupted workflows. Both the database files and the image files, in standard μ Manager file and directory format, are stored in a user-selectable local or remote disk destination ([Figure 1](#)).

To automate slide handling for HCS, we developed a slide management module, SlideLoader, which tracks the slides and either interfaces with a hardware slide loader or, for semi-automatic imaging without the slide loader, prompts the user to place the slide on the stage. SlideLoader can be used multiple times in the same workflow, allowing for loading and imaging slides repeatedly. This design allows for changing image modalities and manual adjustments of the microscope between each imaging pass. Loading slides multiple times may result in possible offsets to the slide position on the stage. To correct for these offsets, we developed modules for calibrating the stage position using the location-invariant edge between the frosted end and the adjacent transparent glass in commercially available slides ([Figures S4](#) and [S5](#)).

Imaging of the slide is performed by the Slidelmager module, which is a wrapper for μ Manager's Multi-D acquisition and thus able to use all capabilities of μ Manager, including selectable light filters and stacks along the z axis. If an area exceeds the size of a single camera snapshot, multiple tiled images are acquired and post-processed with Fiji image stitching to assemble a composite image ([Preibisch et al., 2009](#)) ([Figure 1D](#)). To increase the acquisition rate, we developed a fast custom autofocus plugin ([Figure S6](#)).

In our initial implementation, we developed a workflow and modules optimized for imaging slides containing whole-mount *Drosophila* embryos with gene expression patterns detected by *in situ* mRNA hybridization ([Weizmann et al., 2009](#)). We assembled an HCS microscope platform with a Prior PL-200 slide loader, a

Zeiss Axioplan 2 motorized microscope, a Nikon DSLR D5100 camera, and a Prior motorized stage (Figure 1B). We selected differential interference contrast (DIC) microscopy for capturing both probe staining and sample morphology in a single image, thus making it particularly well suited to high-throughput analysis of tissue or organisms and for studying ontogeny, such as the developing *Drosophila* embryo (Hartenstein and Campos-Ortega, 1997). We designed the workflow to image *Drosophila* embryos with two imaging modalities (Figure S9). For the first pass (Phase 1), we calibrated the microscope for a 5× objective. We ran the workflow to first image manually selected areas of the slide occupied by the coverslip as tiled images, followed by an image analysis module to capture the coordinates of the detected embryos (Figures S7 and S8). After completion of the first pass, we manually adjusted the microscope, moving to a 20× objective, and resumed the workflow at the second entry point (Phase 2). The workflow re-loads the slides and re-images the detected embryos at higher magnification.

To assess the performance, we measured the precision and speed of the imaging process. We manually created imaging objects on slides with a permanent marker, performed the imaging workflow, and manually superimposed the objects. The average displacement was 0.059 μm, about 1.5% of the image at 20× magnification (Figure S5). On average, the tiling at 5× took 2.3 s/image and the detection of twenty-five 20× images, including a focus step, took 12 s/image. At 5× magnification, the slides can be covered with 200–300 tiles, resulting in a rate of about 12 min/ slide. The second-phase high-resolution imaging with 20× magnification takes about 20 min for each 100 detected objects. Imaging the slide with high resolution at 20× would take over 3,000–6,500 images. Thus with approximately 300 embryos per slide, our imaging strategy achieved a more than 10-fold speedup.

To demonstrate OpenHiCamm's ability for autonomously completing an HCS experiment, we used the workflow to image 95 slides made from a 96-well plate experiment (Figure S1). For the low-resolution pass, we selected a slide area with 180 tiles. Low-resolution imaging was completed in about 12 hr or at a rate of 8 min/ slide and yielded 26–751 objects (continuous areas containing one or multiple embryos) per slide. In the second pass, we obtained high-resolution images for embryos with imaging times ranging from 39 min (61 objects with 119 images) to 113 min (334 objects within 573 images) for 90% of the slides excluding those at the tails of the distribution (too few or too many embryos per slide).

For cases that rely only on high-resolution imaging, we developed an additional module, SlideSurveyor, which takes advantage of the camera video feed to rapidly image the slide from live view. We detect objects and re-image with SlidImager. All steps use the same imaging modality, thus limiting alignment problems and user intervention from repeated slide loading. Using SlideSurveyor for Phase 1 at 20× magnification resulted in 20 min/slide, while avoiding slide reloading and changing the objective.

We imaged six additional slides to compare the expression of *Drosophila* embryonic wild-type gene *mirror* (*mirr*) (McNeill et al., 1997) with two intragenic and three intergenic cis-regulatory module (CRM) reporter constructs (Pfeiffer et al., 2008) (Figures 2 and S2). For high-quality slides, our workflow acquired between 75% and 85% of the objects on the slide. One slide (GMR33E04) exhibited age-related degradation (low contrast) and detected only 55% of the total objects on the slide. For each slide, we obtained high-quality images representing six stage ranges and two standard orientations as previously described for manual imaging (Hammonds et al., 2013). The images obtained from slides containing embryos with CRM constructs were compared with the images obtained from slides containing wild-type embryos. The collected images were of sufficiently high resolution to allow identification of distinct elements of the wild-type pattern driven by different CRMs (Figures 2B and S2). These results were comparable with those from similar experiments performed using manual imaging (Pfeiffer et al., 2008).

DISCUSSION

Imaging multicellular samples has become increasingly essential for understanding the complexity of medically relevant biology. To our knowledge, no existing tool is capable of multiple-slide autonomous imaging or adapting studies focused on multicellular samples to HCS. OpenHiCamm adds the abilities to (1) accommodate hardware beyond the microscope itself as demonstrated with the slide loader, (2) handle hardware and software workflows, and (3) track slide contents beyond a single plate/slide setup. To accomplish these goals, we developed a sophisticated task algorithm, capable of resolving hardware and software task dependencies and providing persistence across workflows or interrupted experiments with an SQL database back end. These advances provide the flexibility to adapt workflows currently used for

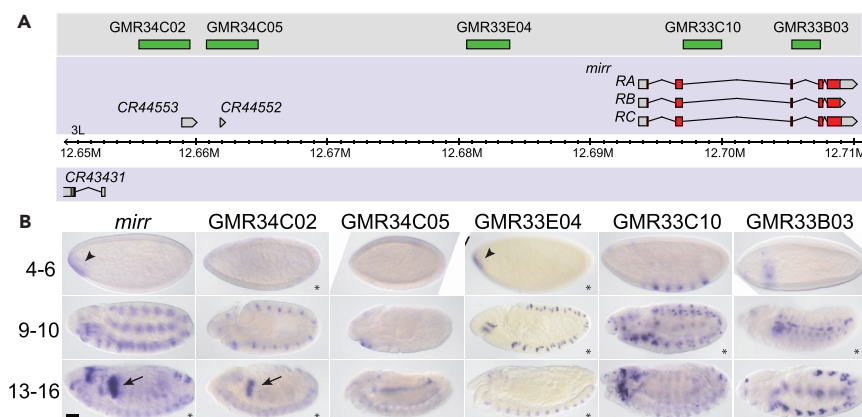


Figure 2. *Drosophila* Embryonic Images Acquired with OpenHiCamm

(A and B) (A) Genomic map of the *mirror* (*mirr*) locus. (B) Expression of the *mirr* gene in embryonic stages 4–6 (blastoderm), 9–10 (gastrulation), and 13–16 (terminal differentiation) visualized by whole-mount *in situ* hybridization with a probe to *mirr* mRNA shown adjacent to the expression produced by the fragments GMR34C02, GMR34C05, GMR33E04, GMR34C02, and GMR34C05. Transgene expression is visualized by whole-mount *in situ* hybridization with a probe to *GAL4* mRNA. Lateral views are shown, anterior to the left.

Expression in the foregut anlage in *statu nascendi* (AISN) is indicated by arrowheads, and expression in the proventriculus is indicated by arrows. Segmental expression apparent at stage 9–10 in the wild-type *mirr* embryos is detectable at stage 4–6 in GMR33C10. Eight images (marked with an asterisk) are composite stitched images from overlapping tiled ROIs. Scale bar, 50 μ m.

See also [Figure S2](#).

HCS, and material science samples, as well as allow integration of experimental devices, such as flow cells activated by changes computationally recognized in an acquired image.

Imaging cells in 96-well plates is well supported, both commercially and by open source products ([Singh et al., 2014](#)). OpenHiCamm expands HCS to sample types for which there is no current solution while providing a robust, self-contained package and a transparent user interface, similar to the Fiji bioimaging package and commercial imaging and microscopy software (e.g., Opera/Operetta by Perkin Elmer). Previously existing tools are implemented as macro packages with only a subset of our software's capabilities ([Edelstein et al., 2010](#)), or are dependent on external software such as LabView ([Conrad et al., 2011](#)). As an important advance over a previous workflow design ([Eberle et al., 2017](#)) implemented in KNIME ([Berthold et al., 2009](#)), our software enables experiments for a high-content screen on multiple slides or multi-well plates. The commercial Metafer Slide Scanning platform is closest in capabilities but is dependent on a single hardware setup and is solely aimed toward histology content at lower resolutions. Magellan utilizes μ Manager and serves as a complementary utility for exploration of single-slide 3D samples or could conceivably be adapted as powerful plugin to our software.

Object recognition has been the primary focus of previous works ([Conrad et al., 2011](#); [Eberle et al., 2017](#); [Tischer et al., 2014](#)) but is only a relatively insignificant part of our software. We tried to avoid the domain specificity of machine learning by creating an intentionally simple but more generalizable object recognition algorithm, while allowing users to add their own recognition pipeline developed in ImageJ/Fiji and pasted as a macro. More sophisticated machine learning algorithms are easily added with a simple programming interface. In fact, the well-supported KNIME software ([Berthold et al., 2009](#)) would make a highly complementary plugin to our software for complex image processing workflows to detect specific features in biological samples.

Our workflow framework is robust, flexible, easily adapted, and extendable to other high-throughput robotics tasks that are increasingly common in modern biology, making the OpenHiCamm package uniquely positioned to provide a foundation for sophisticated high-throughput screens.

METHODS

All methods can be found in the accompanying [Transparent Methods supplemental file](#).

SUPPLEMENTAL INFORMATION

Supplemental Information includes Transparent Methods, 14 figures, and 4 tables and can be found with this article online at <https://doi.org/10.1016/j.isci.2018.03.017>.

ACKNOWLEDGMENTS

We are indebted to the members of BDGP for their support and advice. We thank Richard Weizmann for conducting the whole-mount *in situ* hybridization experiments. We thank Stephan Preibisch for providing implementation for the autofocus function and Abdelrahman Elbashandy for prototype testing. We thank Korneel Hens and Bart Deplancke at Laboratory of Systems Biology and Genetics (LSBG) of Ecole polytechnique fédérale de Lausanne for the full-length cDNA clone of *mirror*. The work was supported by NIH grants R01 GM076655 to S.E.C. and R01 GM097231 to E.F. Work at LBNL was conducted under Department of Energy contract DEAC02-05CH11231.

AUTHOR CONTRIBUTIONS

B.W.B. developed the workflow manager, C.M. developed the hardware integration, K.B. developed the C++ adapter for the PL-200 slide loader, W.W.F. and A.S.H. conducted the biological experiments, and E.F. conceived the workflow manager and supervised the work. A.S.H., S.E.C., and E.F. wrote the manuscript.

DECLARATION OF INTERESTS

The authors declare no competing interests.

Received: November 27, 2017

Revised: February 8, 2018

Accepted: March 2, 2018

Published: April 27, 2018

REFERENCES

- Berthold, M.R., Cebon, N., Dill, F., Gabriel, T.R., Kötter, T., Meinel, T., Ohl, P., Thiel, K., and Wiswedel, B. (2009). KNIME - the Konstanz information miner: version 2.0 and beyond. *SIGKDD Explor. Newsl.* *11*, 26–31.
- Boutros, M., Heigwer, F., and Laufer, C. (2015). Microscopy-based high-content screening. *Cell* *163*, 1314–1325.
- Conrad, C., Wunsche, A., Tan, T.H., Bulkescher, J., Sieckmann, F., Verissimo, F., Edelstein, A., Walter, T., Liebel, U., Pepperkok, R., et al. (2011). Micropilot: automation of fluorescence microscopy-based imaging for systems biology. *Nat. Methods* *8*, 246–249.
- Eberle, J.P., Muranyi, W., Erfle, H., and Gunkel, M. (2017). Fully automated targeted confocal and single-molecule localization microscopy. *Methods Mol. Biol.* *1663*, 139–152.
- Edelstein, A., Amodaj, N., Hoover, K., Vale, R., and Stuurman, N. (2010). Computer control of microscopes using microManager. *Curr. Protoc. Mol. Biol. Chapter 14*, Unit14 20.
- Hammonds, A.S., Bristow, C.A., Fisher, W.W., Weizmann, R., Wu, S., Hartenstein, V., Kellis, M., Yu, B., Frise, E., and Celniker, S.E. (2013). Spatial expression of transcription factors in *Drosophila* embryonic organ development. *Genome Biol.* *14*, R140.
- Hartenstein, V., and Campos-Ortega, J.A. (1997). *The Embryonic Development of Drosophila melanogaster*, Second Edition (Springer-Verlag Berlin).
- Lein, E.S., Hawrylycz, M.J., Ao, N., Ayres, M., Bensinger, A., Bernard, A., Boe, A.F., Boguski, M.S., Brockway, K.S., Byrnes, E.J., et al. (2007). Genome-wide atlas of gene expression in the adult mouse brain. *Nature* *445*, 168–176.
- Levsy, J.M., and Singer, R.H. (2003). Gene expression and the myth of the average cell. *Trends Cell Biol.* *13*, 4–6.
- McNeill, H., Yang, C.H., Brodsky, M., Ungos, J., and Simon, M.A. (1997). *Mirror* encodes a novel PBX-class homeoprotein that functions in the definition of the dorsal-ventral border in the *Drosophila* eye. *Genes Dev.* *11*, 1073–1082.
- Pfeiffer, B.D., Jenett, A., Hammonds, A.S., Ngo, T.T., Misra, S., Murphy, C., Scully, A., Carlson, J.W., Wan, K.H., Laverty, T.R., et al. (2008). Tools for neuroanatomy and neurogenetics in *Drosophila*. *Proc. Natl. Acad. Sci. USA* *105*, 9715–9720.
- Pinkard, H., Stuurman, N., Corbin, K., Vale, R., and Krummel, M.F. (2016). Micro-Magellan: open-source, sample-adaptive, acquisition software for optical microscopy. *Nat. Methods* *13*, 807–809.
- Pitrone, P.G., Schindelin, J., Stuyvenberg, L., Preibisch, S., Weber, M., Eliceiri, K.W., Huisken, J., and Tomancak, P. (2013). OpenSPIM: an open-access light-sheet microscopy platform. *Nat. Methods* *10*, 598–599.
- Pollet, N., Muncke, N., Verbeek, B., Li, Y., Fenger, U., Delius, H., and Niehrs, C. (2005). An atlas of differential gene expression during early *Xenopus* embryogenesis. *Mech. Dev.* *122*, 365–439.
- Preibisch, S., Saalfeld, S., and Tomancak, P. (2009). Globally optimal stitching of tiled 3D microscopic image acquisitions. *Bioinformatics* *25*, 1463–1465.
- Schindelin, J., Arganda-Carreras, I., Frise, E., Kaynig, V., Longair, M., Pietzsch, T., Preibisch, S., Rueden, C., Saalfeld, S., Schmid, B., et al. (2012). Fiji: an open-source platform for biological-image analysis. *Nat. Methods* *9*, 676–682.
- Singh, S., Carpenter, A.E., and Genovesio, A. (2014). Increasing the content of high-content screening: an overview. *J. Biomol. Screen.* *19*, 640–650.
- Tabara, H., Motohashi, T., and Kohara, Y. (1996). A multi-well version of *in situ* hybridization on whole mount embryos of *Caenorhabditis elegans*. *Nucleic Acids Res.* *24*, 2119–2124.
- Tischer, C., Hilsenstein, V., Hanson, K., and Pepperkok, R. (2014). Adaptive fluorescence microscopy by online feedback image analysis. *Methods Cell Biol.* *123*, 489–503.
- Weizmann, R., Hammonds, A.S., and Celniker, S.E. (2009). Determination of gene expression patterns using high-throughput RNA *in situ* hybridization to whole-mount *Drosophila* embryos. *Nat. Protoc.* *4*, 605–618.
- Zanella, F., Lorens, J.B., and Link, W. (2010). High content screening: seeing is believing. *Trends Biotechnol.* *28*, 237–245.

ISCI, Volume 2

Supplemental Information

OpenHiCamm: High-Content Screening

Software for Complex Microscope

Imaging Workflows

Benjamin W. Booth, Charles McParland, Keith Beattie, William W. Fisher, Ann S. Hammonds, Susan E. Celniker, and Erwin Frise

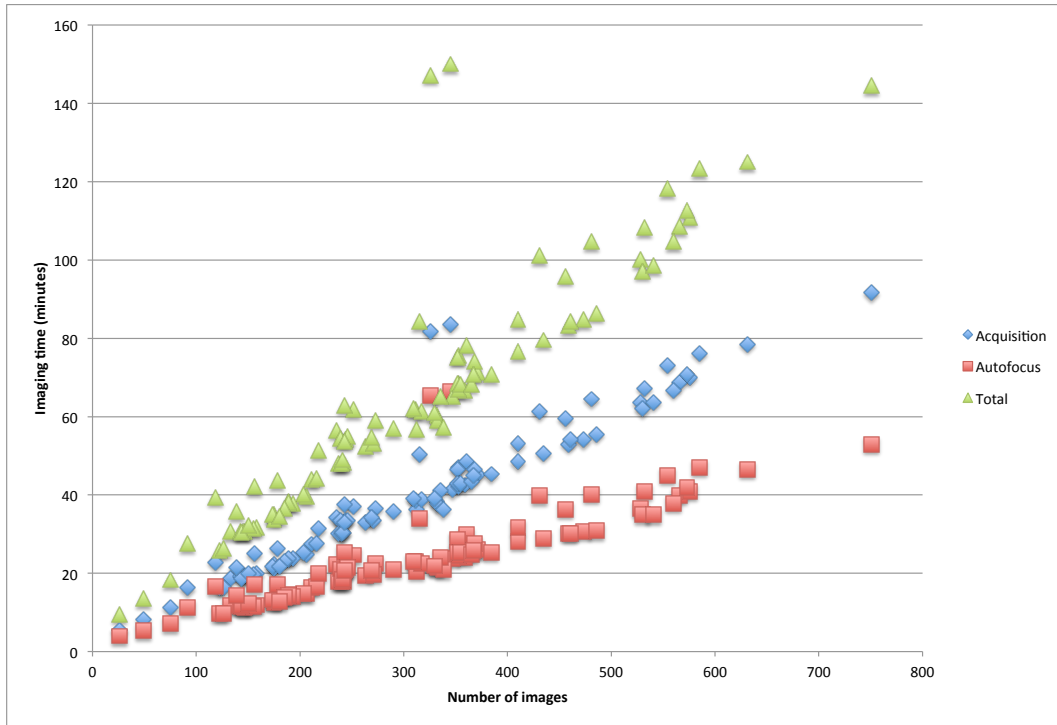


Figure S1. Times for imaging 95 slides from a 96-well experiment with *Drosophila* embryo samples, Related to Figure 1. The time in minutes is shown on the vertical axis, the number of images on the horizontal axis. The 90% percentile, i.e. 5% to 95% are between 119 and 573 images. Acquisition times vary according to the success of the autofocus process.

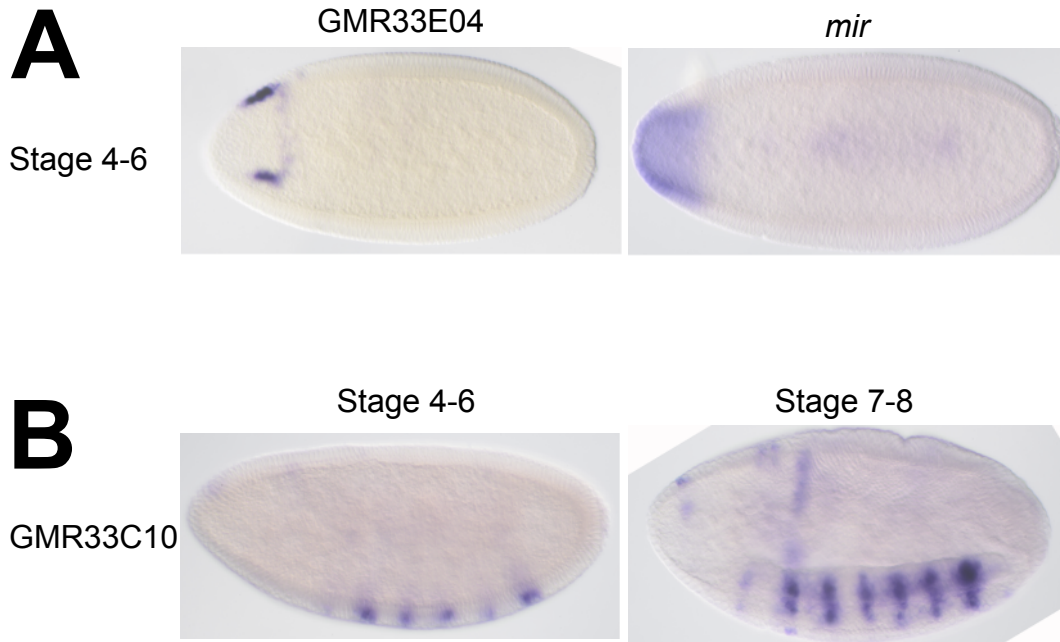


Figure S2. Additional supporting images for the *mirror (mir)* CRM experiment, Related to Figure 2. (A) GMR33E04 and wild-type *mir* expression shown at stages 4-6 from ventral. Wild-type exhibits a continuous pattern whereas GMR33E04 has two smaller expression domains at the boundaries of the wild-type gene expression. (B) GMR33C10 expression at stages 4-6 continues in a segmentally repeated pattern at stages 7-8.

Module name	Module function	Hardware control
SlideLoader	Slide management, loading slides or prompting user to place slide on stage	optional robotic slide loader
SlideImager	Imaging of a slide	Robotic stage, optional Z-axis and illumination/filters
SlideSurveyor	Fast low resolution imaging of a slide using live video feed from camera	Robotic stage
BDGPROIFinder	Region of interest detection	none
CustomMacroROI Finder	Region of interest detection with Fiji/ImageJ macros	
ImageStitcher	Registration and stitching of adjacent images	none
refImager	Imaging a reference position	Robotic stage
compareImager	Capturing set of tiled images around reference position defined in refImager	none
PosCalibrator	Computational comparison of reference images and comparison images and adjustment of position list.	none

Table S1. List of implemented modules and their functions for OpenHiCamm, Related to Figure 1.

Transparent Methods

OpenHiCAMM workflow manager, data model and module management

OpenHiCAMM is written in the Java 1.8 programming language as a plugin for μ Manager 1.4.x. While compatible with the basic ImageJ and μ Manager distribution, for image processing, we require the extended and standardized plugin selection provided by Fiji. At its core is a custom workflow manager providing following functionality: 1) A common interface for modules implementing either hardware control or image processing tasks; 2) Configuration of a modularized workflow and module specific parameters; 3) Resolving dependencies and ordered execution of the modules; 4) Metadata and image storage management; 5) Response to events from the hardware; and 6) A graphical user interface for designing workflows, configuring storage and modules and starting/stopping and resuming workflows.

OpenHiCAMM itself is platform agnostic but μ Manager hardware support depends on the operating system. We developed and tested the C++ code for PL200 slide loader hardware adapter on Macintosh OSX 10.10 (or newer) also tested it under Linux.

The source code is available on Github (<https://github.com/bdgp/OpenHiCAMM>).

Data model

The OpenHiCAMM workflow engine manages two types of data, a set of execution tasks and the module and task configurations (Figure S3).

Execution tasks: Each task represents a single unit of work. The purpose of a task is 1) to allow the system to schedule module executions and 2) to provide a record of successful or unsuccessful module completion. Tasks are connected to each other using a directed acyclic graph. A workflow task may be started once all of its parent tasks have completed successfully. Workflow modules may tag tasks as serial or parallel. Serial tasks are completed in sequential order, and are suitable for hardware dependent tasks such as slide loading and imaging. Parallel tasks can be run simultaneously and are suitable for image processing or analysis. Each task consists of a unique task identification number, its current status, and its associated module. Tasks are connected together in parent-child relationships. The task workflow is similar to the concept of a data dependency graph that is common in many workflow execution systems (Zaharia, Chowdhury et al. 2010).

Workflow module and task configurations: Metadata for configurations are stored as key-value pairs. Workflow module configurations are parameters set by the user and can be accessed by all tasks in the module. Module configurations are used for configuring parameters that apply to all tasks within the module. Task configurations apply to each task individually. Task configurations are not manually entered by the user, but are generated by the module. The task configuration is used to store information about which item of work each task is to perform. For example, the SlideLoader task configuration stores the identification and location for the slide to load, the SlideImager task configuration stores the identification of the image to be acquired by that task.

Images are part of the task data and not explicitly handled. OpenHiCamm directs the μ Manager acquisition engine to store images in its native format to a workflow dependent location and tracks imaging through the task sets.

Workflow implementation and API

System architecture

The OpenHiCamm workflow engine is designed to store its data in a SQL database backend. Our current version implemented HSQLDB (<http://hsqldb.org>) as database backend. We chose HSQLDB because it is implemented in pure Java and can be distributed as a cross-platform JAR file, making installation using the Fiji update manager much easier.

Each workflow module can create a configuration entry and one or more tasks. Upon invocation of a configured workflow, a new workflow instance with a task list is generated, tasks linked as acyclic graph and task information stored in the database. The workflow manager iterates through all pending tasks and executes every task not completed and with no dependency on preceding tasks or competing for the microscope hardware.

Each workflow can have multiple distinct phases. Each phase is named by its initial module, the topmost module in the graph. The user selects which phase to execute in the workflow dialog. Providing multiple phases and allowing the user to select between them gives the user the opportunity to split a workflow into sections and perform any required manual adjustments between each phase. For example, in our workflow designs, we expose two phases; the first performs a low-resolution scan and searches for regions of interest. The second performs a high-resolution tiled imaging of each region of interest found in the first phase.

For tasks tagged as “Serial”, child tasks will inherit task configuration from parent tasks. This allows a form of communication between parent and child tasks in the same workflow phase. For workflows split into separate phases, it may be desirable to pass information from the first phase tasks to the second phase tasks. This cannot be done using task configuration since the second phase tasks are not directly related to the first phase tasks. For these cases, the user can create custom database tables and add identifying information to each record so that the second phase modules can find the associated data. We use this approach in our workflow to pass the position list produced by the region of interest finder in phase 1 of our workflow to the phase 2 imaging module.

Modules have been optimized for robustness and rapid processing and acquisition. For modules interfacing with hardware, we added abstractions and modifications to the call sequence to catch aberrant hardware behavior and communication errors. The module will attempt to correct problems or skip the current step before stopping and reporting errors the user. Our improvements vastly increased the robustness of the stock μ Manager software and resulted in requiring user interaction only for hardware problems.

Module API

OpenHiCamm is designed to be easily extensible using modules. Custom modules need to implement OpenHiCamm’s module interface. Our Module interface allows user-created modules to customize the behavior of their modules using at several key entry points (Table S2).

Each module can provide a custom configuration user interface (UI). For the configuration UI, a module developer needs to implement a configure method and return a Configuration object (Table S3). If the module is part of the workflow, the UI will be automatically displayed in the tabbed configuration dialog (Figure S10). The configuration object will be managed and stored in the database by the workflow manager.

To add a new module, a module designer needs to add a Java jar file in the `openhicamm_modules/` directory. On startup, OpenHiCamm will automatically detect and load all jar files in the `openhicamm_modules/` directory, and the module will be available in the Workflow Design interface. Module designers are free to design their own database tables, or use the provided configuration object for storing configuration metadata. A thin, easy-to-use wrapper around the popular ORMLite SQL object relational mapping library (<http://ormlite.com>) is provided in the Connection and Dao classes.

Reporting interface

OpenHiCamm includes a reporting interface, which the module designer can extend to provide custom workflow reports (Table S4). We have used this reporting interface to successfully detect and correct implementation bugs and hardware issues in our workflow designs. By clicking the “View Reports” button in the Workflow Dialog, the Report Dialog is displayed with a drop-down list of the reports available for viewing. Module designers can build custom reports by implementing the Report interface and including the report in their plugin JAR file. The report will automatically be detected and added to the list of available reports.

Reports are created by interfacing with the OpenHiCamm workflow manager to query the state of the workflow, and producing HTML output for display. To produce HTML with a convenient Java based interface, we included a HTML templating library named “Tag”. Our Report UI uses the JavaFX WebView component to display the HTML document. JavaScript code can be added to the HTML document. We used JavaScript to interface the report with the microscope hardware, to allow for loading a slide and positioning the stage to a previously imaged object. Once the document is created, it is stored in the workflow directory, and can be re-generated at any time by the user.

Example workflow module implementation for detecting objects of interest

We implemented an ROI Finder module that executes an image processing pipeline to return an ImageJ ROI list with objects of interest (see section “ROI Finder and *Drosophila* embryo detection”). We used our workflow, μ Manager and Fiji data structures to integrate the output of the ROI Finder in a second phase workflow:

The ROI Finder module creates a position list of ROIs and stores it in a custom SlidePosList database table. In the first phase, the SlideImager module processes user defined SlidePosList to determine which areas of the slide will be imaged. In the subsequent phases, SlideImager processes the most recently added SlidePosList records. SlideImager computes if a region of interest is larger than the size of a single image and creates a set of partially overlapping tile positions.

The position list JSON schema defined by μ Manager allows for custom properties to be added to each position in the position list. The ROI Finder module adds the “stitchGroup” custom

property to each position in the ROI tileset to group the individual tiles together. The SlideImager module looks for custom properties in the position list and converts them into task configuration records. Because task configuration is inherited from parent to child for serial tasks, the downstream ImageStitcher module will use the “stitchGroup” task configuration to determine which images need be stitched together.

Core modules

SlideLoader module SlideLoader is responsible for initializing the slide loader hardware, keeping track of which slides are loading and unloading slides to and from the stage. SlideLoader defines a high-level programming interface with hardware dependent libraries, similar to the current μ Manager model. We developed a sample hardware library for a Prior PL-200 slide loader that supports most microscopes and is able to hold and handle up to 200 slides.

SlideImager module SlideImager is a wrapper for the μ Manager Multi-D dialog and acquisition engine, primarily providing configuration storage in the SQL database and invoking the the acquisition engine with the previously configured parameters. The position list can be either manually predefined or the result of a previous workflow module, such as ROIFinder. To manually create a position list, we use the μ Manager position list user-interface to define a region on the slide. SlideImager will pass configured parameters from the Multi-D dialog and the position list to the Multi-D acquisition engine. All functions provided by the Multi-D dialog are available, able to use all abilities of the μ Manager, including selectable light filters and stacks along the Z axis. We added a custom hook to the Multi-D acquisition engine, linking back to SlideImager, to track the acquisition of each image and schedule post-acquisition image processing tasks.

Calibration of the slide position on the stage

We developed the PosCalibrator module to processes images from a dedicated instance of SlideImager (Figure S4). Both modules can be optionally inserted into the workflow, after the slide is loaded onto the stage. SlideImager records images at an invariant position and PosCalibrator matches the slide position to a previous reference image and adjusts a position list to detected shift.

After loading a slide the first time, using the standard SlideImager module (called refImager in the example workflow in Figure S9), the user creates a position list with on entry containing the approximate position of the area where the slide frosting and the corner intersect. At each slide, when the workflow reaches SlideImager, the user-defined area is imaged and stored as reference (Figure S4A). At workflows that load the slide again, optionally at different magnification, the user can create an instance of a modified SlideImager module with additional functionality for re-imaging the area in case of an interrupted workflow (called compareImager in Figure S9), followed by PosCalibrator. SlideImager images the same area again and the images are matched to previously acquired images in the module PosCalibrator, Figure S4B.

While sophisticated scale and rotation invariant methods have been described, they are generally slow or hard to implement. For PosCalibrator, we created a fast and robust pipeline based on Generalized Hough Transform (GHT) template matching. GHT matches the edge

contours between a template and a target image by counting matching pixels in an accumulator (Ballard 1981). For each boundary point of the template, we pre-computed an R-table with the coordinate differences $x_c - x_{ij}$ and $y_c - y_{ij}$ between a fixed reference x_c/y_c in the middle and each boundary point x_{ij}/y_{ij} . To account for rotation and scaling we also pre-computed scaled and rotated x/y boundary pairs and stored them in the R-table. For each entry in the R-table, we calculated the gradient $\phi(\mathbf{x})$. For each pixel in the search image, we matched the pixel gradient to ϕ and increased the a corresponding entry in an accumulator array. The accumulator entry with the maximum value corresponds to the position of the template in the search image.

We customized an existing ImageJ plugin, GHT (<http://rsb.info.nih.gov/ij/plugins/ght/index.html>), and used the code in a new plugin to encapsulate the pipeline to process and return matched image coordinates as ImageJ ROI. The pipeline converts images to grayscale, resizes them and uses the ImageJ IsoData algorithm find two thresholding values for the reference and all combined calibration images. The threshold values are used to generate binary images, the images undergo morphological processing to eliminate holes and errant pixels. From the set of calibration images the pipeline selects an image containing the both slide frosting and slide border at roughly equal proportions. The reference image and the selected calibration image are converted to edge contours (Figure S4C) for matching with the GHT algorithm (Figure S4D). The workflow module PosCalibrator calls the plugin and transforms the matched image coordinates to stage coordinates. GHT is scale and rotation invariant but, to further reduce running time, we adjust the image sizes to the same dimensions with user configurable parameters (e.g. 4 for matching 5x and 20x magnifications). Image pixel translations to stage movements were measured with the μ Manager Pixel Calibration plugin and the resulting values entered as configuration parameters and used to adjust the offset. We tested the modules both with DIC and fluorescent illumination. If no matches are found, a warning message is added to the log and imaging continued with no calibration.

We tested our system with manual markings and found negligible displacements (Figure S5). Our slide calibration works both with light and fluorescent microscope systems.

Slide Surveyor

The SlideSurveyor module is similar to the SlideImager in that it takes as its input a position list and acquires images but does not use Micro-Manager's Multi-D acquisition module. Instead, SlideSurveyor sets the camera to “Live Mode”, moving to each position in the list, acquiring a live mode image. The image is then copied into an image buffer representing the entire slide. “Live Mode” captures video, which allows quickly acquiring low-resolution images without triggering the camera's shutter. Running the acquisition in “Live Mode” allows the SlideSurveyor to quickly map out an entire slide, even at 20x magnification. SlideSurveyor can image the contents of an entire slide in 20 minutes, as opposed to several hours with the Multi-D module and individual images. The resulting images are low quality, but sufficient for ROI detection. The same “Live View” mode is also used to accelerate our custom autofocus engine. The ability to survey an entire slide using the 20x lens enabled us to avoid using a two-phase workflow, helping the workflow to complete more quickly, and providing more accurate positioning and centering of the ROIs when performing the second phase.

Autofocus

We created a plugin, FastFFT (Figure S6), using the μ Manager autofocus API. In FastFFT, we perform the Fast Fourier Transform (FFT) using the Mines Java Toolkit (<http://inside.mines.edu/~dhale/jtk/>) and apply a bandpass filter to the power spectrum. The logarithmic values between the two percentage radiuses are summed up and the process repeated for all images in the same stack. The image with the highest value is selected. Empirically we determined the best bandpass filter between 15 and 80 percent to place the focal point in the middle of the embryo (Figure S6C). The bandpass filter values can be adjusted in the configuration dialog. To accelerate the image acquisition process, our autofocus module changes the camera setting to live imaging with reduced image size.

We compared FastFFT to two μ Manager autofocus implementations, J&M and Oughtafocus, by measuring the plugin reported level of detail at multiple stage positions for 10 embryos. The FastFFT module performed as designed and returned highest scoring focal planes at the middle of the embryos (Figure S6A and S6C). The μ Manager functions returned optimal focal planes with more variability, depending on the stage of the embryo (Figure S6A). At early embryos, focal planes were visually indistinguishable and within 6 μ m of each other, less than the thickness of the cell-layer surrounding the blastoderm. At later stages, the μ Manager functions tended to focus on the surface of the embryo (Figure S6C). FastFFT performed a magnitude faster than the μ Manager function (Figure S6B), an average of 40 seconds for scanning 100 positions, compared to 206 seconds (Oughtafocus) and 246 seconds (J&M). Moreover, FastFFT was more consistent in its speed.

To further speed up processing and cover a wide range of focal planes, we perform a coarse focusing with large interval steps and a broad range and second a finer granularity focusing with small interval steps around the previous best focal plane. Both intervals are user configurable as part of the graphical configuration dialog. We configured it to take 41 images at 10 μ m intervals and 7 images at 3.3 μ m intervals. To prevent hardware damage caused by a potential slow drift in measurements, we also added a configuration for an absolute maximum/minimum Z position that cannot be exceeded. The plugin has a configurable counter to skip focusing on a selected number of images. The counter is reset every time after two consecutive images match the same Z position after completing the autofocus function. This prevents erroneous focusing on occasional mis-detected objects such as air bubbles.

ROIFinder and *Drosophila* embryo detection

This module processes single images and returns regions of interest (ROI). It provides a high level interface that returns an object's bounding box and can be easily adjusted to custom image processing pipelines. We developed two computationally efficient ROIFinder implementations. Both We developed two computationally efficient custom ROIFinder implementations and macro based implementation, CustomMacroROIFinder, which allows the user to simply paste a previously developed ImageJ macro into a dialog and execute it as part of the workflow. CustomMacroROIFinder is extremely flexible and along with the powerful Fiji UI and macro

recording abilities allows for the development of complex segmentation workflows by users less experienced with image processing.

The custom implementations segment the image, use Fiji's "Analyze Particles" function to detect and measure segmented areas and store the bounding boxes for areas exceeding a selectable minimum size. We set the Analyze Particles function to discard objects at the image boundaries. Virtually all objects missed in our *Drosophila* embryo imaging experiment were discarded for crossing image boundaries rather than failure to detect the object.

The simpler ROIFinder variant segments the object by automatic thresholding with IsoData and is suitable for uniform samples distinct from background such as fluorescent labeled samples.

For our work with *Drosophila* embryos we developed a variant that uses the texture, which is frequently inherent in biological samples (Figure S7). Our pipeline calls Fiji edge detection, applies a threshold on the edge image with a fixed, empirically determined value (13, out of 255 gray values) and performs morphological image operations (close, fill holes) to smoothen the areas. This pipeline will be suitable for histological samples and other whole mount specimens.

For the SlideSurveyor workflow, we used the CustomMacroROIFinder (Figure S8). We developed a macro that 1) removes horizontal and vertical lines that were a result of SlideSurveyor's image stitching with Fiji's FFT Bandpass filter plugin, 2) resize, 3) convert to a mask, 4) thresholds the image, 5) performs morphological operations and, 6) applies the "Analyze Particles" function as described before.

ROIFinder provides a standard API for a image processing pipeline as well as the ability to execute a macro and using Fiji's image processing plugins, programming and macro recording abilities, a customized pipeline can be easily implemented. More complex samples such as mutant embryos with altered developmental phenotypes can be detected and rapidly imaged at high resolution for computational analysis. We envision users building sample specific object detection pipelines, which can significantly increase the throughput if uninteresting objects can be discarded at low resolution.

***Drosophila* embryo imaging workflow**

Our two phase workflow is shown in Figure S9. After loading the slides, our SlideImager module captures images with a given list of positions on the slide. The initial position list is configured by the user as the maximum area of interest and slides are imaged in overlapping tiles at 5x magnification. Captured images are processed with a module, ROIFinder, to detect objects and their coordinates stored in the database. Detected objects are stored as bounding boxes, transformed to the imaging area and the content of the bounding boxes imaged again at higher resolution (Figure S1 and S2). If a bounding box exceeds the size of a single image at 20x, multiple tiled images are acquired and post-processed with a module, ImageStitcher, using an Fiji stitching algorithm (Preibisch, Saalfeld et al. 2009) to assemble a composite image (Figure 1D, Figure S2).

The Fiji based stitching worked reliably for 2-3 images but failed frequently for large composites with 3 or more images. We found these large composites containing dense clusters of overlapping embryos and discarded the results.

User interface

The main window is available from the μ Manager plugin menu (Figure 1). The user can select a local or remotely mounted (NFS or CIFS) directory as location for the workflow database, settings and images.

Using a workflow editor, the user can add and arrange modules from an existing set to create a workflow (Figure S9). For our low/high magnification implementation, we created a combined workflow with two imaging phases. The first imaging phase arranges the SlideLoader, refImager, SlideImager and ROIFinder modules, the second imaging phase arranges compareImager, PosCalibrator, another instance of SlideImager and ImageStitcher. Modules for the second imaging phase will automatically detect and use results from the first imaging phase. When the workflow reaches a point with no child tasks, it will terminate.

The “Start Task” in the main window defines the entry point, in our implementation, either the first or second imaging phase.

Each workflow module can be configured with persistent settings in a configuration dialog called from the main window (Figure S10-S12). The SlideLoader module creates a pool of slides with the current slides in the robotic slide loader, allows for scanning the slides and adding meta-data information (Figure S10). The SlideImager module will call the μ Manager Multi-D dialog for configuration of the slide imaging task and save the settings in the workflow database (Figure S13). SlideImager’s derived modules, refImager and compareImager, are configured similarly. refImager takes a reference image for calibration at a user defined position. compareImager captures an overlapping set of images centered around the user defined position of RefImager. Upon successful completion both refImager and the set of compareImager images are used by the PosCalibrator to identify the matching position (see Detection of the slide position) and adjust the position coordinates. The ROIFinder module can be configured to record objects of a user defined minimum size and tested on images in the configuration dialog (Figure S12). Testing the ROI finder opens a window with images for each intermediate processing step and the resulting bounding boxes as illustrated in Figure S7 and S8.

For each defined workflow, new instances are used for processing a pool of slides. Thus, the same basic configuration can be used for multiple slide pools. Image files are stored in μ Manager format in a folder set by the initial workflow configuration and sub-folders matching the workflow instance and workflow tasks, respectively.

The workflow progress is stored in a SQL database. For debugging or correcting unexpected problems, the Workflow Dialog includes a “Show Database Manager” button that opens a graphical database querying interface with the workflow database loaded. The OpenHiCamm source also includes a “sqltool” command-line script which, when run in the workflow directory, opens a command-line SQL query tool, which is useful for debugging purposes.

Reviewing the results

During workflow processing, progress can be monitored with a live imaging view and a log window (Figure S13). Workflows can be stopped and resumed at defined checkpoints. Upon completion, results can be visualized in an HTML report.

At the conclusion of the pipeline, OpenHiCamm generates a summary report, displaying the calibration images, and the results for all imaging passes. The report is generated as an html file (Figure S14) and rendered in OpenHiCamm in a report window. In OpenHiCamm, the report viewer allows for loading slides and positioning the stage to positions. The report file can also be independently opened and viewed in a standard web browser.

In situ hybridization experiments

We performed in situ hybridizations as previously described (Weiszmam, Hammonds et al. 2009). We collected and hybridized wild type embryos with an RNA probe made from a cDNA clone of mirror and used a probe that detects Gal4 reporter RNA to hybridize embryos of five *Drosophila* strains, GMR33C02, GMR33C05, GMR33E04, GMR33C10, GMR33B03, from the Janelia Farm Research Campus (JFRC) FlyLight Gal4 collection (Pfeiffer, Jenett et al. 2008), each carrying a putative mirror enhancer with a Gal4 reporter.

Embryos were mounted on slides and imaged with OpenHiCamm. Resulting images were cut out and rotated with Adobe Photoshop for publication.

Supplemental Figures

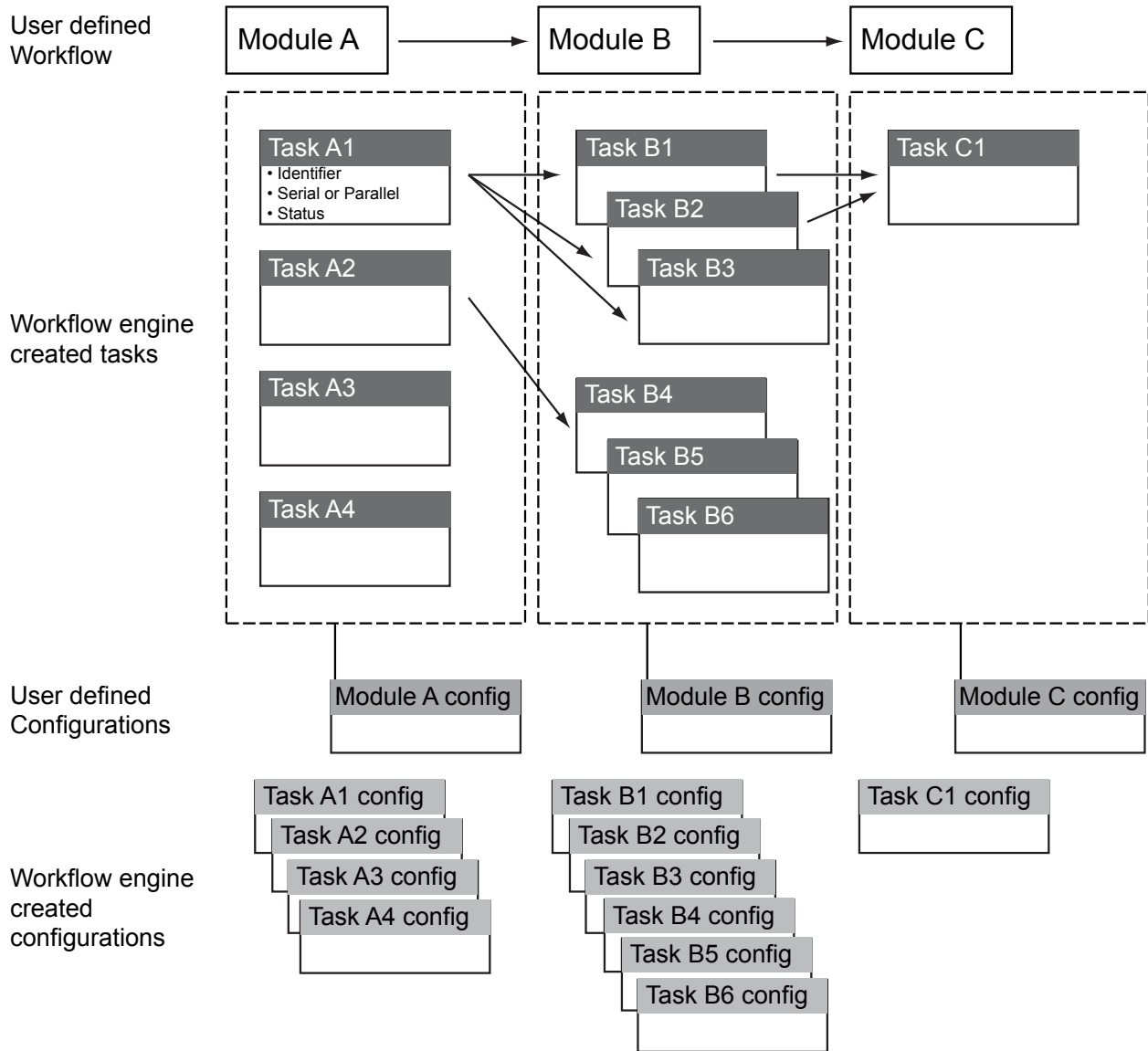


Figure S3. OpenHiCamm data model, Related to Figure 1. Shown are three modules, labeled A, B, C with module specific tasks (labeled A1, A2, A3 for module A, etc.), module configurations and task configuration entries. The user defines the workflow and the module configurations, the workflow engine creates the tasks and the task configurations (left).

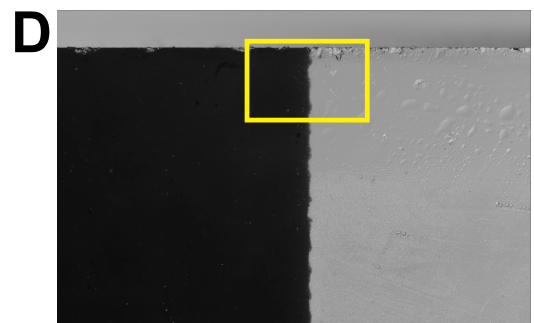
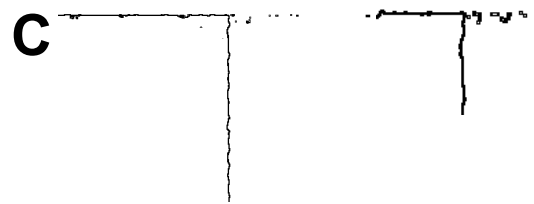
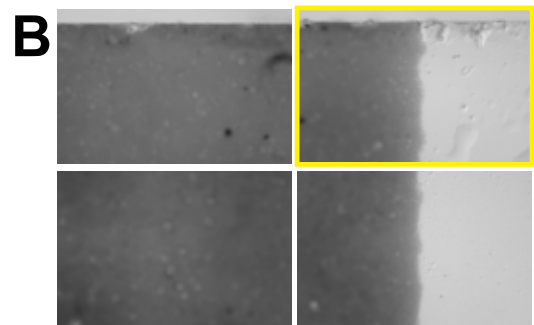
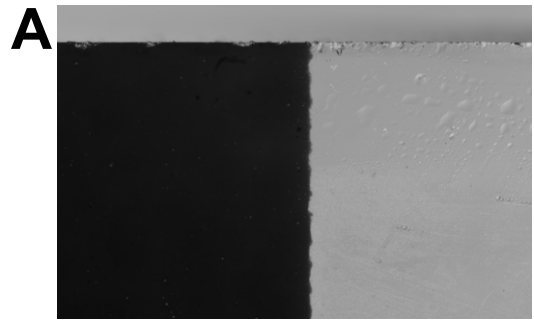


Figure S4. Alignment calibration for the same slide, loaded twice and imaged at different magnifications, Related to Figure 1. (A) Image at 5x magnification at position defined by the user. **(B)** Tiled images at 20x magnification around the original position of (A). The automatically selected calibration image is framed in yellow. **(C)** Edge images of (A) and (B) that are used for GHT. **(D)** Position of the calibration image in the reference image shown with a yellow box.

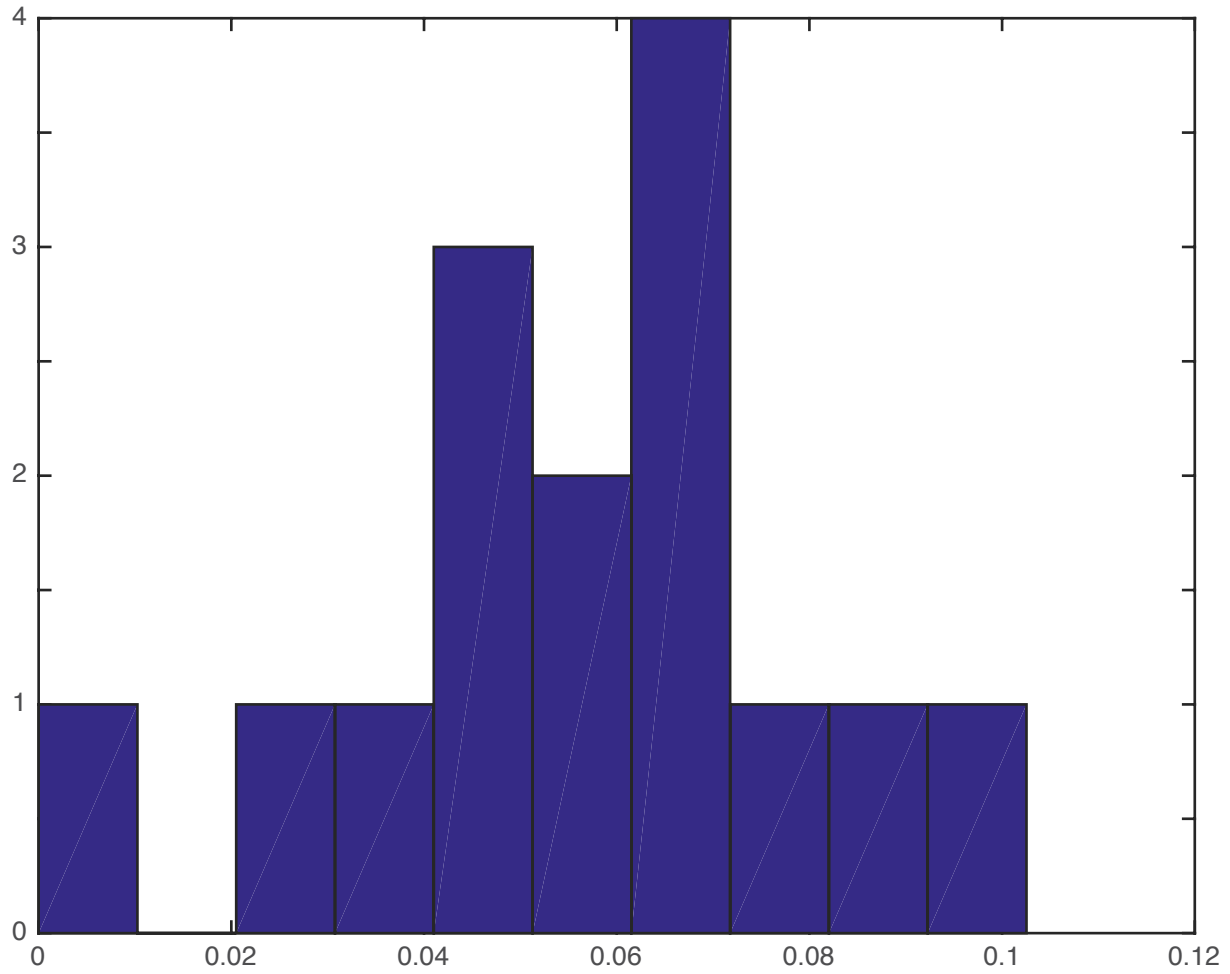


Figure S5. Precision of detecting same objects after calibrating slides, Related to Figure 1. Histogram depicts the euclidean distance between the position of 10 objects in μm .

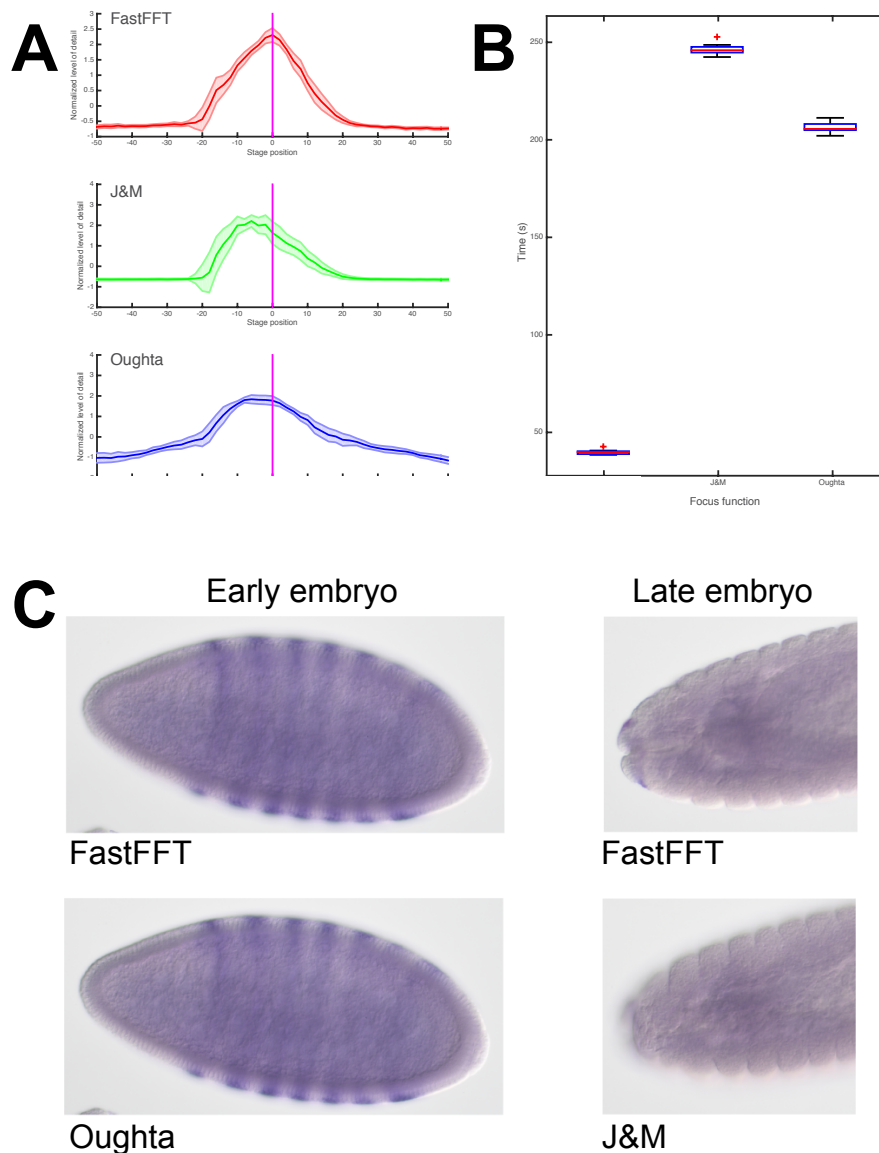


Figure S6. Autofocus performance of FastFFT compared to μ Manager's J&M and OughtaFocus function (at default setting), Related to Figure 1. (A) Median and standard deviation of normalized values returned from each plugin at stage positions -50 μ m to +50 μ m. Values reported by the autofocus functions were normalized as z-scores (centered to have mean 0 and scaled to have standard deviation 1). FastFFT is shown in red, J&M in green and OughtaFocus in blue. The stage positions for all three plugins are centered around the best value return for FastFFT. J&M shows the largest variance. **(B)** Box plot showing the execution times for the three plugins for the 100 sampled stage positions. **(C)** Early blastoderm embryo (left) and late embryo (right) showing the highest scoring focal planes for FastFFT (top) compared to OughtaFocus and J&M (bottom). Results show little discernible difference for the early embryo but a focal plane in the middle of the embryo for FastFFT compared to a focal plane on the surface for J&M.

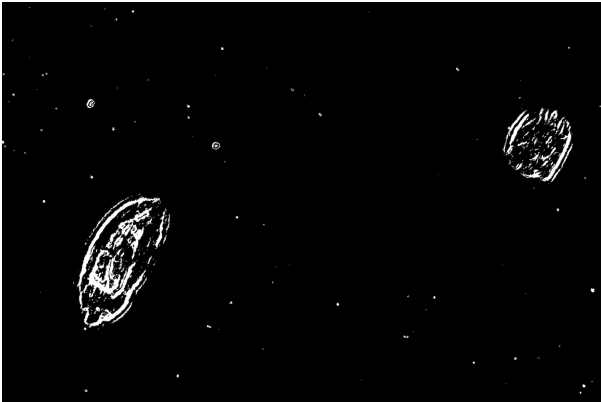
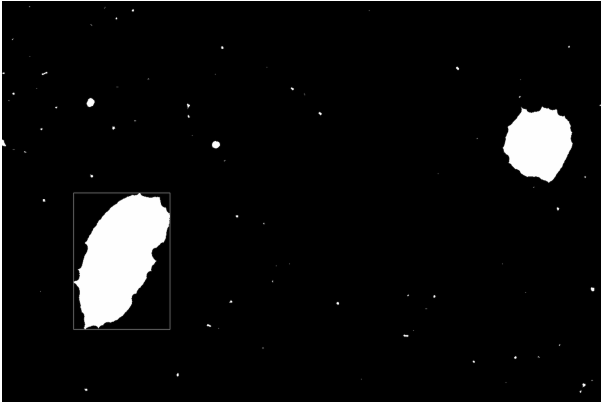
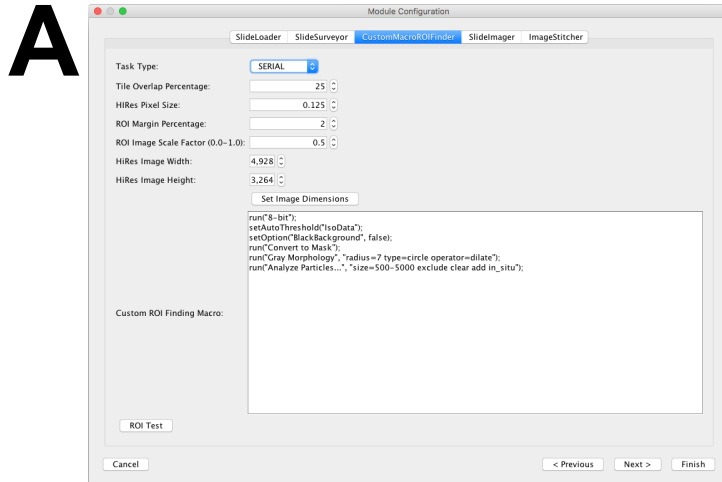
A**B****C**

Figure S7. Visualization of results for the ROIfinder module, Related to Figure 1. (A) Image at 5x magnification with embryos. (B) Edge detection. (C) Detected ROI, shown as black object masks.



B

```
// SlideSurveyor PostProcessing
run("Bandpass Filter...", "filter_large=25 filter_small=15 suppress=Vertical tolerance=5 autoscale saturate");
run("Bandpass Filter...", "filter_large=25 filter_small=15 suppress=Horizontal tolerance=5 autoscale saturate");

// resize 0.5
run("Scale...", "x=0.5 y=0.5 width=4329 height=3629 interpolation=Bilinear average create");

// CustomMacroROIfinder Custom ROI Finding Macro
run("8-bit");
setAutoThreshold("IsoData");
setOption("BlackBackground", false);
run("Convert to Mask");
run("Gray Morphology", "radius=7 type=circle operator=dilate");
run("Analyze Particles...", "size=500-5000 exclude clear add in_situ");
```

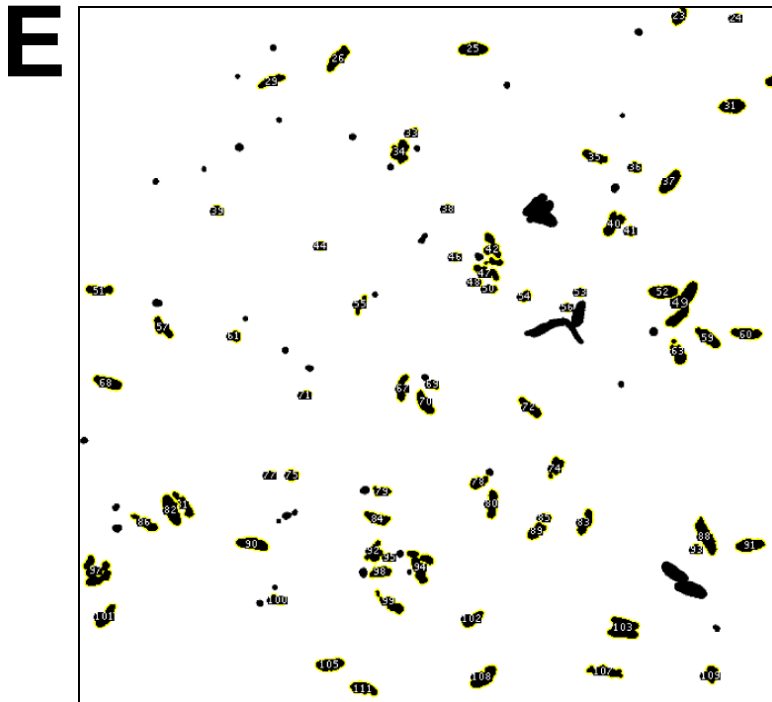
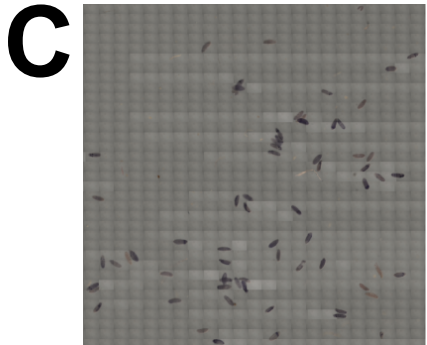


Figure S8. CustomMacroROIfinder for Drosophila imaging, Related to Figure 1. (A) Configuration dialog with text box for custom macro. **(B)** Macro used for *Drosophila* imaging workflow. **(C)** Excerpt of the stitched slide from SlideSurveyor. **(D)** Image in panel C after applying FFT Bandpass filter. **(E)** Result after thresholding, morphology and particle detection.

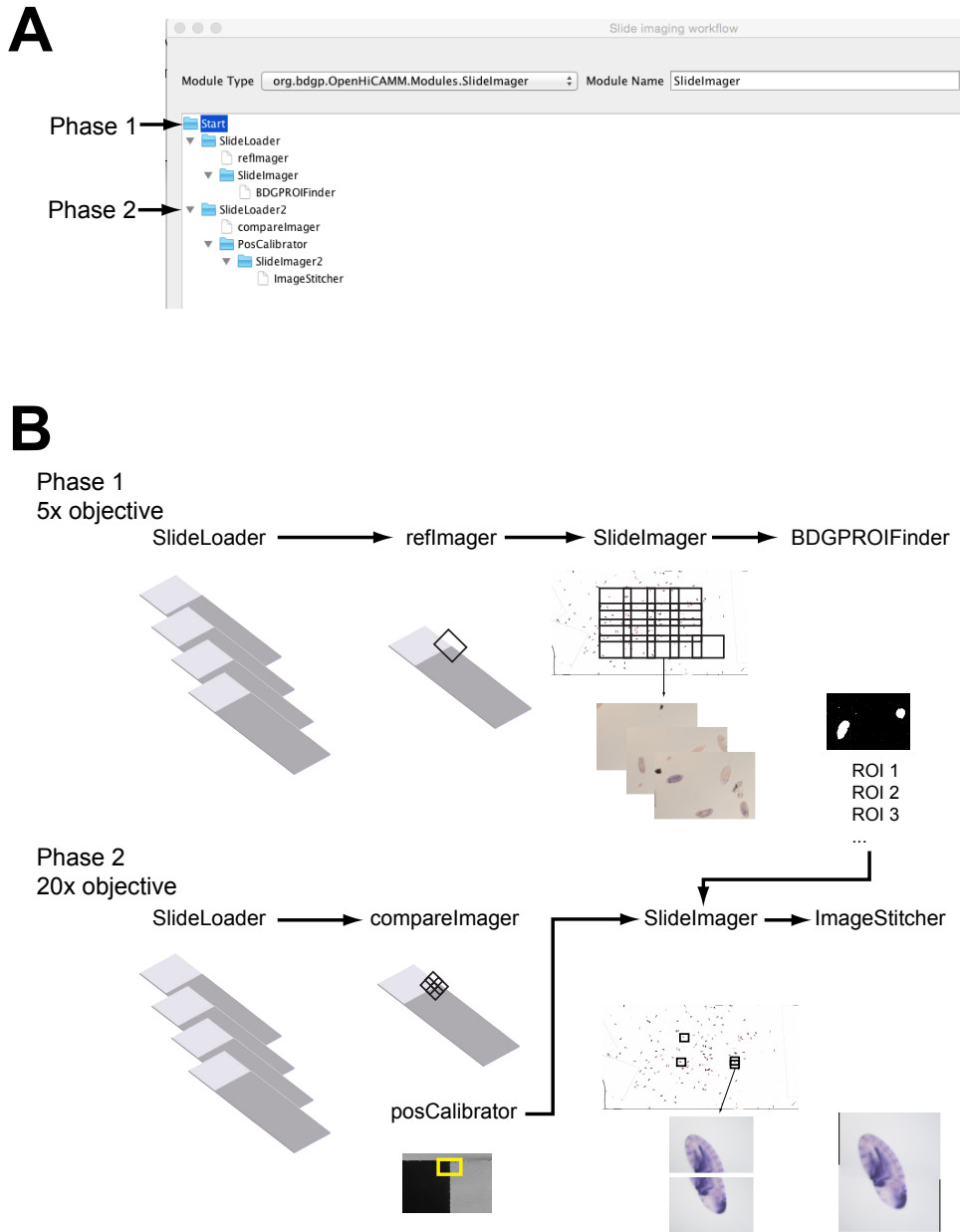


Figure S9. Workflow for Drosophila imaging, Related to Figure 1. Shown is the 5x/20x magnification configuration used for imaging Drosophila embryos. **(A)** Configuration dialog with the workflow arranged in a tree-like structure. Child modules display a higher level of indentation than the parent modules. The workflow execution starts at Phase 1 or 2 entry points and stops when it reaches a point with no further child modules. **(B)** Schematic representation of the workflow. Phase 1 of the workflow loads a slide (SlideLoader), takes a reference image for calibrating the slide position on the stage (reflmager), images the slides in overlapping tiles (SlideImager), detects ROIs and stops. Phase 2, configured as second entry point, loads the same slides a second time (SlideLoader), calibrates the position list by taking images around the reference images and finding a matching position (comparelmager), images the ROIs from the first workflow (SlideImager) and, if necessary, stitches adjacent images (SlideStitcher).

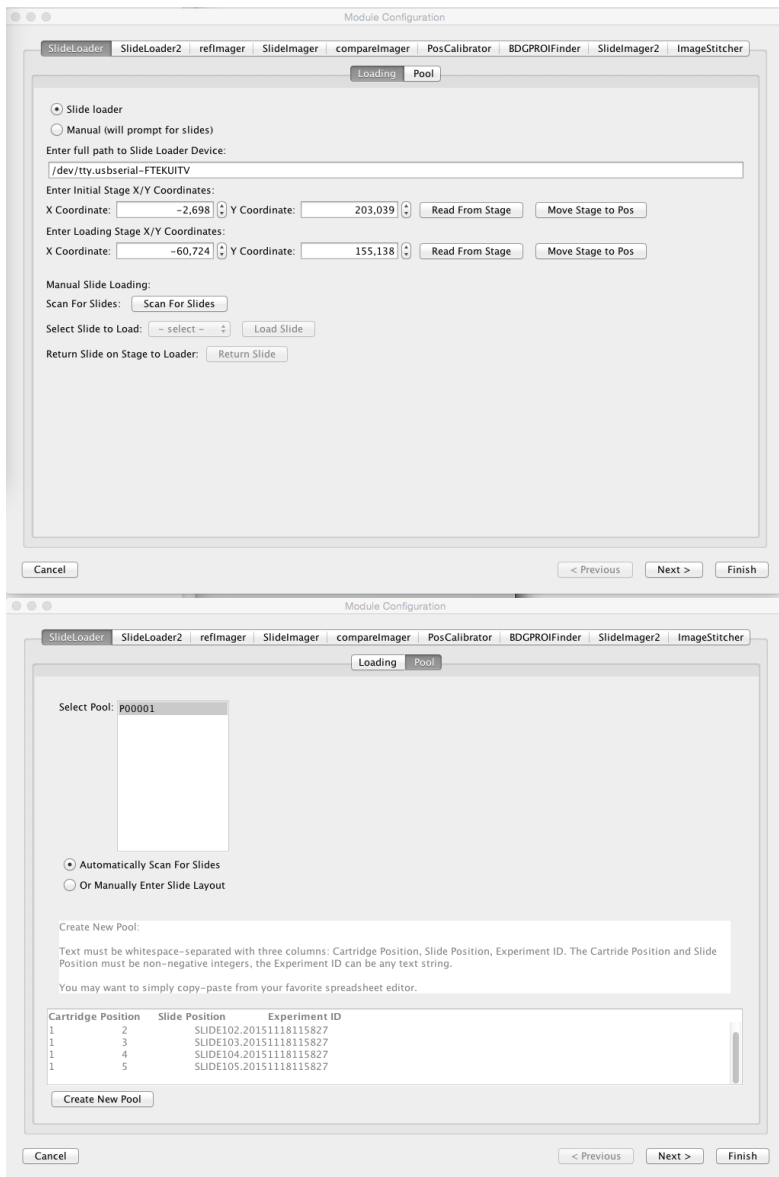


Figure S10. Dialog for module configurations, Related to Figure 1. Configurations for the SlideLoader module are shown. Top of the dialog shows a tabbed list for each module in the workflow, remaining part of the dialog shows the currently selected tab. **(Top)** Basic configuration options for the hardware. For robotic loading of slides, the stage needs to be moved to a position matching the slide loader and the position can be defined here. **(Bottom)** Definition for the metadata of the slide pool. Each slide in the slide loader (a row in the dialog) is located in a cartridge and a position in that cartridge and can be assigned with a descriptive entry.

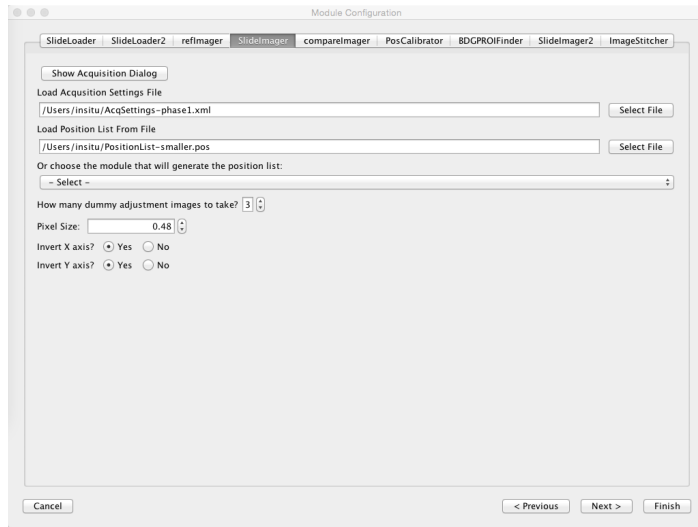


Figure S11. Dialog for module configurations, Related to Figure 1. Shown is the SlideImager. Settings can be configured and saved with the μ Manager Multi-D dialog (button “Show acquisition dialog”), settings from the Multi-D dialog can be assigned, and a user defined position list or a previously computed position list selected. We found some cameras needed time to adjust to the light. Thus we added a configuration option to take a selectable number of “dummy” images before starting the imaging. The pixel size needs to be calibrated with μ Manager and entered as configuration to adjust the pixels in the images to the stage position. We also added options to invert the coordinates for the stage compared to the captured image, if necessary.

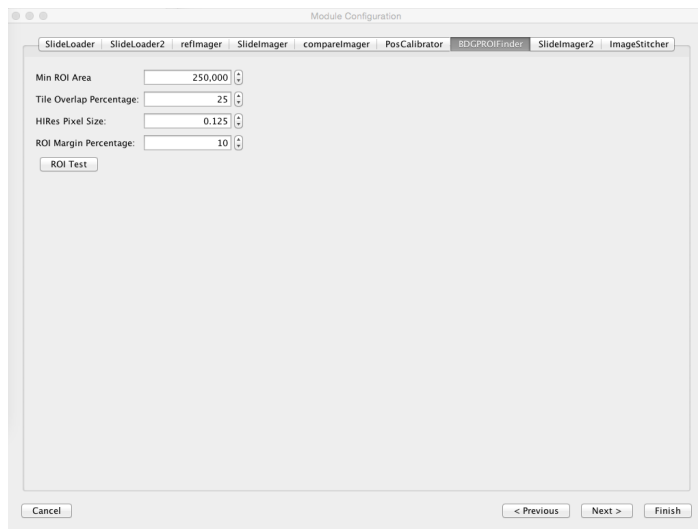


Figure S12. Dialog for module configurations, Related to Figure 1. Shown is our ROIFinder module. The ROIFinder requires a configuration for a minimum size of an object to be recorded (top line), the overlap to adjacent images, the pixel size (Figure G) and a configurable increase for the detected bounding box size.

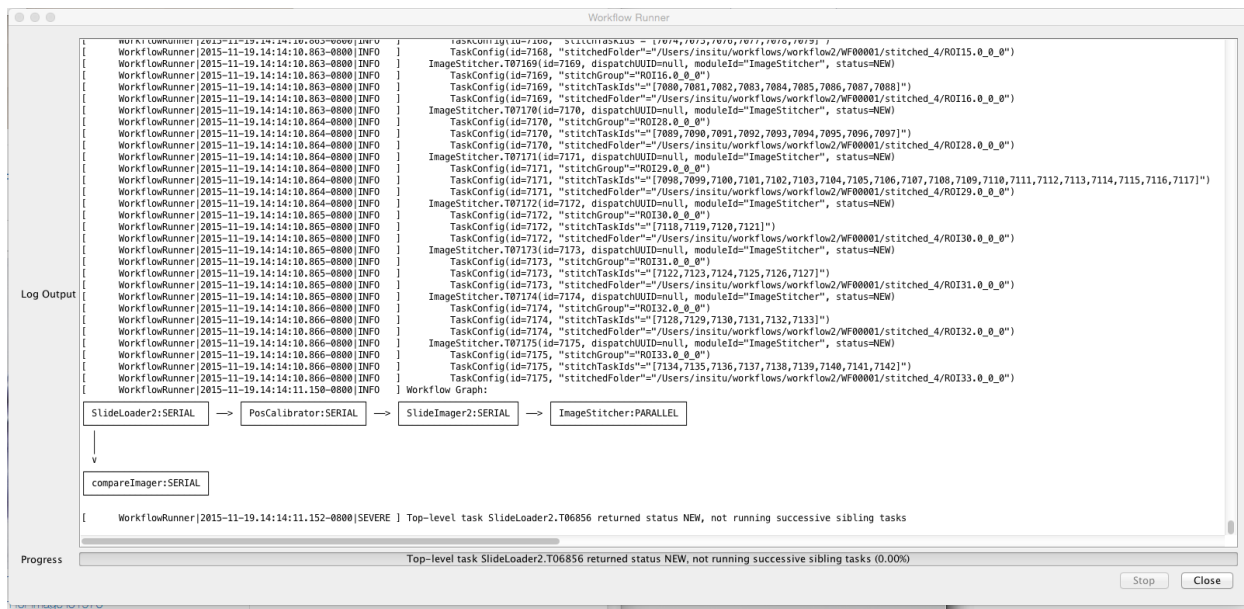


Figure S13. Log output during running the workflow, Related to Figure 1. Initially the workflow manager computes all tasks to complete the currently configured workflow and adds them to the persistent database. The workflow manager displays the currently configured workflow and the tasks that need to be completed sequentially because of hardware dependencies (“SERIAL”) or can be executed in parallel (“PARALLEL”), usually only those modules dependent on computations. Progress for each task is printed as log messages, and the overall progress and remaining time shown in a progress bar (bottom).

Image Image(id=192, slideld=1, channel=0, slice=0, frame=0, position=191, acquisitionId=2), ROI ROI(id=75, imageld=192, x1=2452, y1=448, x2=3088, y2=1412)

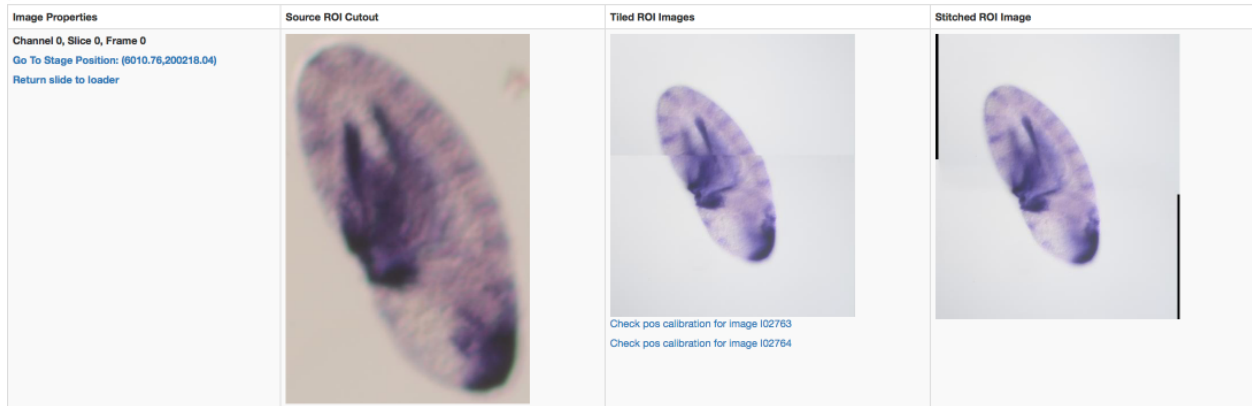


Image Image(id=192, slideld=1, channel=0, slice=0, frame=0, position=191, acquisitionId=2), ROI ROI(id=76, imageld=192, x1=2108, y1=2296, x2=2984, y2=3196)



Figure S14. Summary report after acquisition, Related to Figure 1. Shown is a screenshot from the browser. Hyperlinks on the left allow for loading the slide and positioning at the location of the object. The images on the left are from low resolution (5x) phase 1, middle are composite of roughly tiled (according to coordinate position) high resolution phase 2 images (20x), and right composite images showing the result of the image stitching module.

Supplemental Tables

API call	Functionality
initialize	Called during the workflow initialization phase, before module configuration. Allows the module to perform any required initialization.
configure	Called when the user performs the module configuration step. This method returns a Configuration object which handles the configuration UI display, and serialization of configuration options to the database.
createTaskRecords	Creates a database record for each task that is expected to be run during the workflow. Called before the start of the workflow run.
runInitialize	A second initialization entry point. This point is called before each workflow run, whereas initialize is called only once per module.
run	The actual workflow module execution code. Called once per task.
cleanup	Task cleanup code. Is called even if the tasks throws an exception. Called immediately after the run method completes.
setTaskStatusOnResume	Allows customization of the task status when the workflow is run in "Resume" mode.

Table S2. Module API and functions, Related to Figure 1. Custom modules need to implement the shown functions in order to work as OpenHiCamm workflow module.

API call	Functionality
retrieve	Returns the list of configuration key-value pairs retrieved from the configuration UI
display	When given a list of configuration key-value pairs, display returns a Swing Component that contains the configuration UI, with the configuration applied
validate	Scans the configuration UI for any validation errors, and returns a list of ValidationError objects, which is displayed to the user.

Table S3. Module configuration user interface API and functions, Related to Figure 1.

API call	Functionality
initialize	Pass in the WorkflowRunner context object and perform any required initialization steps.
runReport	Run the report and return the contents of the report as an HTML string.

Table S4. Report interface API and functions, Related to Figure 1.

Supplemental References

Ballard, D. H. (1981). "Generalizing the Hough transform to detect arbitrary shapes." *Pattern recognition* **13**(2): 111-122.

Pfeiffer, B. D., A. Jenett, A. S. Hammonds, T. T. Ngo, S. Misra, C. Murphy, A. Scully, J. W. Carlson, K. H. Wan, T. R. Lavery, C. Mungall, R. Svirskas, J. T. Kadonaga, C. Q. Doe, M. B. Eisen, S. E. Celniker and G. M. Rubin (2008). "Tools for neuroanatomy and neurogenetics in *Drosophila*." *Proc Natl Acad Sci U S A* **105**(28): 9715-9720.

Preibisch, S., S. Saalfeld and P. Tomancak (2009). "Globally optimal stitching of tiled 3D microscopic image acquisitions." *Bioinformatics* **25**(11): 1463-1465.

Weiszmann, R., A. S. Hammonds and S. E. Celniker (2009). "Determination of gene expression patterns using high-throughput RNA in situ hybridization to whole-mount *Drosophila* embryos." *Nat Protoc* **4**(5): 605-618.

Zaharia, M., M. Chowdhury, M. J. Franklin, S. Shenker and I. Stoica (2010). "Spark: Cluster Computing with Working Sets." *HotCloud* **10**: 10-10.